PHYSICAL REVIEW E **89**, 012302 (2014)

Effect of concentration polarization on permselectivity

Ramadan abu-Rjal,[1] Vahe Chinaryan,[1] Martin Z. Bazant,[2] Isaak Rubinstein,[1] and Boris Zaltzman[1]
[1]*Jacob Blaustein Institutes for Desert Research, Ben-Gurion University of the Negev, Sede Boqer Campus 84990 Israel*
[2]*Department of Chemical Engineering and Department of Mathematics, Massachusetts Institute of Technology, Cambridge, Massachusetts 02139, USA*
(Received 21 August 2013; published 6 January 2014)

In this paper, the variation of permselectivity in the course of concentration polarization is systematically analyzed for a three-layer membrane system consisting of a nonperfectly permselective ion exchange membrane, homogeneous or heterogeneous, flanked by two diffusion layers of a binary univalent electrolyte. For a heterogeneous membrane, an ionic transport model is proposed, which is amenable to analytical treatment. In this model, assuming a constant fixed charge in the membrane and disregarding water splitting, the entire transport problem is reduced to solution of a single algebraic equation for the counterion transport number. It is concluded that for both types of membrane the concentration polarization may significantly affect the permselectivity of the system through the effects of the induced nonuniformity of the coion diffusion flux in the membrane (convexity of the coion concentration profile) and varying membrane-solution interface concentration. While the former is significant for low membrane fixed charge density, for a heterogeneous membrane, the latter might be considerably affected by the flux focusing effect at the permeable membrane segments.

DOI: 10.1103/PhysRevE.89.012302 PACS number(s): 82.45.Gj, 47.61.Fg, 82.39.Wj, 82.45.Mp

I. INTRODUCTION

Concentration polarization (CP) is an electrochemical term pertaining to the effects of formation of ionic concentration gradients [1] in an electrolyte solution adjacent to a permselective (charge-selective) surface (an electrode, an ion-exchange membrane, or an array of nanochannels in a microfluidic system) upon the passage of a dc current. CP results from diffusional limitation, that is, a concentration gradient develops so that the diffusion flux of coions rejected by the ion-exchange membrane compensates the electromigration flux caused by the applied potential [2,3]. Intuitively speaking, the formation of concentration gradients should result in saturation of the current density caused by the vanishing of the interface concentration; when the current tends to its limiting value, the potential drop over the system tends to infinity. Nevertheless, in real ion-exchange systems, the limiting current density can be considerably exceeded. In practice, what is commonly viewed as the expression of CP is the characteristic nonlinear shape of an experimentally measured steady-state voltage-current (VC) curve: a low-current linear (Ohmic) region is followed by current saturation at the "limiting" value, corresponding to vanishing interface concentration, which is in turn followed by an inflection of the VC curve and the transition to the "overlimiting" conductance (OLC) regime.

The mechanism of OLC remained unclear for a long time, and still is a subject of intense research [4–14]. We will not address this issue in the current study. Instead, we focus on a much simpler issue: variation of the overall counterionic transport number in the course of CP in general and of the CP in electrolyte diffusion layers, in particular. The ionic transport number, defined as the proportion of a particular ionic flux in the overall current density, is a major transport characteristic of a permselective system. For a perfect binary system, when the entire current through the membrane is carried by the counterions only, their transport number equals unity (and so the coion transport number is zero). For a nonperfect system the counterion transport number lies between one-half and unity.

In the membrane literature, confusion has existed for a long time about this notion. On the one hand, it is perfectly well recognized that the ionic transport numbers in a membrane system depend on the transport regime [15]. On the other hand, quite commonly the overall transport numbers are employed as material characteristics, on a par with the membrane thickness, fixed charge density, porosity, etc., as if they were independent of the regime of operation, e.g., of the magnitude of the electrical current passed through the system [2,16–18]. This might originate from the classical seminal study of CP by Spiegler [2], in which the assumption of constant counterion transport number independent of the current was used in the boundary condition at the membrane-solution interface.

In this paper, we embark on sorting out this confusion through a systematic analysis of the CP effect on the counterionic transport number in homogeneous and heterogeneous membranes, focusing on purely electrostatic aspects (in the spirit of recent micro- and nanochannel studies in which the transport in a nanochannel is modeled directly [19]); thus, we disregard the water splitting and possible variations of the membrane charge in the course of CP [6,7,14]. We begin in Sec. II with the analysis of a simple one-dimensional (1D) three-layer setup consisting of a nonperfectly permselective homogeneous ion-exchange membrane flanked by two diffusion layers of a univalent binary electrolyte. From there, we proceed in Sec. III to generalizing this analysis for a heterogeneous membrane. As a by-product, we come up with a simple 2D model of steady-state ion transfer through a nonperfect heterogeneous membrane amenable to analytic treatment. Technically speaking, the entire problem is reduced to solving a single algebraic equation for the ionic transport number. This is a considerable generalization of the previous one-layer 2D models of heterogeneous membranes assuming perfect permselectivity [20,21]. Finally, we point out that the fluid through flow, important in micro- and nanofluidic contexts (Refs. [19,22] is negligible for dense nonporous ion-exchange electrodialysis membranes addressed here, and, thus, is left beyond the scope of this study.

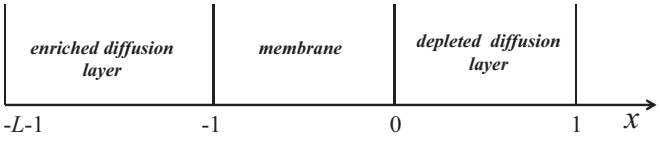

FIG. 1. Sketch of three-layer setup for a homogeneous cation exchange membrane.

II. HOMOGENEOUS CATION-EXCHANGE MEMBRANE

In this section we address a simple 1D three-layer problem, modeling CP in an imperfectly permselective membrane flanked by two univalent binary electrolyte diffusion layers of different thicknesses bordered by two stirred bulk liquids (Fig. 1). The corresponding model problem in the dimensionless form reads

$$c_x^+ + c^+\varphi_x = j^+ = \text{const}, \quad c_x^- - c^-\varphi_x = j^- = \text{const}; \quad (1)$$

$$c = c^+ - N(x) = c^-, \quad N(x) = N[H(x+1) - H(x)]; \quad (2)$$

$$c(-L-1) = 1, \quad c(1) = 1; \quad (3)$$

$$\varphi(-L-1) = 0, \quad \varphi(1) = -V. \quad (4)$$

Here c^+ and c^- are the dimensionless concentrations of cations (counterions) and anions (coions), respectively (notations with tildes are used below for the dimensional variables, as opposed to their untilded dimensionless counterparts), normalized by the outer stirred bulk concentration $\tilde{c}_0$:

$$c^+ = \frac{\widetilde{c}^+}{\widetilde{c}_0}, \quad c^- = \frac{\widetilde{c}^-}{\widetilde{c}_0}, \quad (5)$$

and c is the dimensionless salt concentration. φ and V are the dimensionless electric potential and voltage, respectively, normalized by the thermal potential kT/e:

$$\varphi = \frac{e\widetilde{\varphi}}{kT}, \quad V = \frac{e\widetilde{V}}{kT}. \quad (6)$$

x is the dimensionless spatial coordinate normalized by the thickness of the depleted diffusion layer $\widetilde{l}$, which equals the thickness of the membrane, and L is the dimensionless thickness of the enriched diffusion layer:

$$x = \frac{\widetilde{x}}{\widetilde{l}}, \quad L = \frac{\widetilde{L}}{\widetilde{l}}. \quad (7)$$

N is the dimensionless fixed charge density in the membrane:

$$N = \frac{\widetilde{N}}{e\widetilde{c}_0} \quad (8)$$

and $H(x)$ is the Heaviside step function.

Equations (1) are the steady-state Nernst-Planck equations, where j^+ and j^- are the dimensionless ionic fluxes (with a minus sign; for simplicity, equal ionic diffusivities are assumed, the same for the solution and the membrane) in the depleted diffusion layer, $0 < x < 1$, in the membrane, $-1 < x < 0$, and in the enriched diffusion layer, $-L-1 < x < -1$. Equation (2) is the mean electroneutrality condition held in the membrane and diffusion layers, where $N(x)$ is the fixed charge density (0 in diffusion layers and $N > 0$ in the membrane). The conditions (3) fix the concentrations at the outer edges of the unstirred diffusion layers equal to the concentrations in the stirred bulk (L is the dimensionless thickness of the enriched diffusion layer). Conditions (4) specify the potential drop across the layers; see Fig. 1.

Furthermore, the relevant conditions of continuity at the electrolyte-membrane interfaces, after applying the electroneutrality condition (2), are

$$\begin{aligned}(c_x + c\varphi_x)|_{x=-1-} &= (c_x + [c+N]\varphi_x)|_{x=-1+},\\ (c_x - c\varphi_x)|_{x=-1-} &= (c_x - c\varphi_x)|_{x=-1+};\end{aligned} \quad (9)$$

$$\begin{aligned}(c_x + c\varphi_x)|_{x=0+} &= (c_x + [c+N]\varphi_x)|_{x=0-},\\ (c_x - c\varphi_x)|_{x=0+} &= (c_x - c\varphi_x)|_{x=0-};\end{aligned} \quad (10)$$

$$\begin{aligned}(\ln c + \varphi)|_{x=-1-} &= (\ln[c+N] + \varphi)|_{x=-1+};\\ (\ln c - \varphi)|_{x=-1-} &= (\ln c - \varphi)|_{x=-1+};\end{aligned} \quad (11)$$

$$\begin{aligned}(\ln c + \varphi)|_{x=0+} &= (\ln[c+N] + \varphi)|_{x=0-};\\ (\ln c - \varphi)|_{x=0+} &= (\ln c - \varphi)|_{x=0-}.\end{aligned} \quad (12)$$

Conditions (9) and (10) impose the continuity of fluxes in the electrolyte-membrane interfaces at points $x = -1$ and $x = 0$, respectively; whereas (11) and (12) impose the continuity of the electrochemical potentials at the same points. The proposed "leaky" membrane model [10] is just a version of the classical Teorell-Meyer-Sievers [23,24] or Spiegler [2] model of ionic transport through an ion-exchange membrane.

Substituting the electroneutrality condition (2) into Eq. (1) yields

$$2c_x + N(x)\varphi_x = j^+ + j^- = J, \quad -L-1 < x < 1, \quad (13)$$

$$[2c + N(x)]\varphi_x = j^+ - j^- = I, \quad -L-1 < x < 1. \quad (14)$$

Here $-J$ and $-I$ are the total salt flux and the electrical current density, respectively.

Integrating Eqs. (13) and (14) in the diffusion layers $-L-1 < x < -1$ and $0 < x < 1$ and applying boundary conditions (3) and (4), we easily derive the following expressions for the concentration and electric potential within the diffusion layers:

$$\begin{aligned}c(x) &= 1 + \frac{J}{2}(x+L+1),\\ \varphi(x) &= \frac{J}{I}\ln\left(1 + \frac{J}{2}(x+L+1)\right), \quad -L-1 < x < -1,\end{aligned} \quad (15)$$

$$\begin{aligned}c(x) &= 1 + \frac{J}{2}(x-1),\\ \varphi(x) &= \frac{J}{I}\ln\left(1 + \frac{J}{2}(x-1)\right), \quad 0 < x < 1.\end{aligned} \quad (16)$$

Furthermore, using Eqs. (13) and (14) inside the membrane we obtain

$$2c_x + \frac{NI}{2c+N} = J, \quad -1 < x < 0. \quad (17)$$

Integrating Eq. (17) and applying the continuity of the electrochemical potentials $\mu_+ = \ln c^+ + \varphi$ and $\mu_- = \ln c^- - \varphi$ across the electrical double layers (EDLs) at the electrolyte-membrane interface, Eqs. (11) and (12), results in the following

algebraic equation:

$$\frac{J}{2}=\left[c+\frac{NI}{2J}\ln(2Jc+JN-IN)\right]\Big|_{-1+}^{0-}, \tag{18}$$

where

$$c|_{0-}=-\frac{N}{2}+\sqrt{\frac{N^2}{4}+\left(1-\frac{J}{2}\right)^2}, \tag{19}$$

$$c|_{-1+}=-\frac{N}{2}+\sqrt{\frac{N^2}{4}+\left(1+L\frac{J}{2}\right)^2}. \tag{20}$$

Finally, substituting (19) and (20) into (18) yields the following equation relating I to J:

$$\frac{NI}{J}\ln\left(\frac{J\sqrt{N^2+\left(1+\frac{LJ}{2}\right)^2}-NI}{J\sqrt{N^2+\left(1-\frac{J}{2}\right)^2}-NI}\right)$$
$$=-J+\sqrt{N^2+\left(1-\frac{J}{2}\right)^2}-\sqrt{N^2+\left(1+\frac{LJ}{2}\right)^2}. \tag{21}$$

To derive the voltage-current relation, we notice that in a three-layer system (Fig. 1), the overall voltage drop $V=\varphi|_{x=-L-1}-\varphi|_{x=1}$ is the sum of the electric potential drops across the membrane and two diffusion layers and the potential jumps at the two membrane-solution interfaces, corresponding to the interfacial EDLs, obeying relations (11) and (12). Thus, using (11), (12), (15), and (16) we find

$$V=\frac{J-2c|_{-1+}^{0-}}{N}+\ln\frac{c+N}{c}\Big|_{0-}$$
$$-\ln\frac{c+N}{c}\Big|_{-1+}-\frac{J}{I}\ln\frac{2-J}{2+LJ}. \tag{22}$$

The solution of the algebraic equation (21) in terms of Lambert functions [25] with respect to I, $(0<I<I^{\lim}\underset{N\to 0}{\longrightarrow}\infty)$ for a given J $(0<J<2$, irrespective of $N)$, yields the counterion transport number τ^+,

$$\tau^+\overset{\text{def}}{=}(J/I+1)/2, \tag{23}$$

varying between one-half (for a nonselective membrane) and unity (for a perfect permselective membrane). The calculation is completed by computing the voltage V for a given I through Eq. (22). To characterize the overall effect on permselectivity let us define τ_0 as the equilibrium value of τ^+ at zero current, $\tau_{\lim}$ as the corresponding value at the limiting current, along with $\Delta\tau=\tau_{\lim}-\tau_0$ for the variation of τ^+ in the course of CP. For τ_0 we have from Eq. (21)

$$\tau_0=\frac{1}{2}\left(1+\frac{N}{\sqrt{N^2+4}+2(L+1)}\right). \tag{24}$$

The decrease of τ_0 with increasing L in this expression corresponds to decreasing control by the membrane (the only permselective element) of the ionic fluxes in our system.

Similarly, at the limiting current $J=2$, Eq. (21) yields for $N\gg 1$

$$\tau_{\lim}=\frac{1}{2}+\frac{1}{1+\frac{(1+L)^2}{N}}+O(N^{-2}). \tag{25}$$

We note in this formula the appearance of a characteristic scale $N\sim L^2$ for the CP effect on permselectivity.

In Figs. 2(a)–2(c) we plot the counterion transport number τ^+ versus the salt flux J for varying membrane fixed charge density N and dimensionless thickness of the enriched diffusion layer L. In the inset we present the computed V-J dependence. The limiting value 2 of J corresponds to vanishing of the solute concentration at the depleted interface $x=0$. In Fig. 2(d) we plot τ_0 [Eq. (24)] along with $\tau_{\lim}$, Fig. 2(e), and $\Delta\tau$, Fig. 2(f), for the intermediate range of N.

The strong dependence of the counterionic transport number on J observed in Figs. 2(a)–2(c) is due to the interface concentration variation in the course of CP. When the depleted layer is thicker than the enriched one ($L\ll 1$), a minor increase in the counterionic transport number is observed, due to the increased permselectivity at the depleted side of the membrane [Fig. 2(a)]. When the enriched diffusion layer is thicker than the depleted one ($L\gg 1$), a considerable decrease in the counterionic transport number may occur, due to the increasing asymmetry between the minor gain of permselectivity at the depleted interface and its major loss at the enriched one [Fig. 2(c)]. This CP effect is almost absent in the symmetric case (equal diffusion layer thicknesses $L=1$), unless the membrane permselectivity is poor [Fig. 2(b), lines 2,3 compared to line 1]. The reason is that, as may be easily found through differentiation of Eq. (17), for a decreasing salt concentration depicted in Fig. 3, the salt concentration profile in the membrane is convex:

$$c_{xx}=N(-\varphi_x)_x=-\frac{2NIc_x}{(2c+N)^2}<0,\quad -1<x<0, \tag{26}$$

that is, the salt concentration lies above the corresponding linear profile. Thus, for a membrane with high permselectivity, the electric field in the membrane is nearly constant and the salt profile in the membrane is practically linear. As a result, the gain in permselectivity at the depleted side of the membrane is practically compensated by the corresponding loss at the enriched side. For a poorly permselective membrane, the strong variation of the membrane conductivity, Eq. (17), and the nonconstancy of the electric field result in pronounced convexity of the salt concentration profile in the membrane developing in the course of concentration polarization (see Fig. 3) and yield a decrease in the counterion transport number even for diffusion layers of equal thicknesses.

These observations are summarized in Fig. 2(f): With a thin enriched diffusion layer (plot 1) the initial increase of the $\Delta\tau$ is due to the appearance of permselectivity, increasing with depletion in the course of CP. This rise is followed by decrease towards zero corresponding to perfect permselectivity at $N\gg 1$, Figs. 2(d) and 2(e). With symmetric diffusion layers (plot 2) the initial decrease of $\Delta\tau$ is due to convexity of the membrane salt concentration profile, disappearing upon the increase of N. Finally, with a thick enriched layer (plot 3) the initial $N=O(1)$ decrease of $\Delta\tau$ due to the combined effect of convexity (disappearing for $N\gg 1$) and loss of permselectivity due to

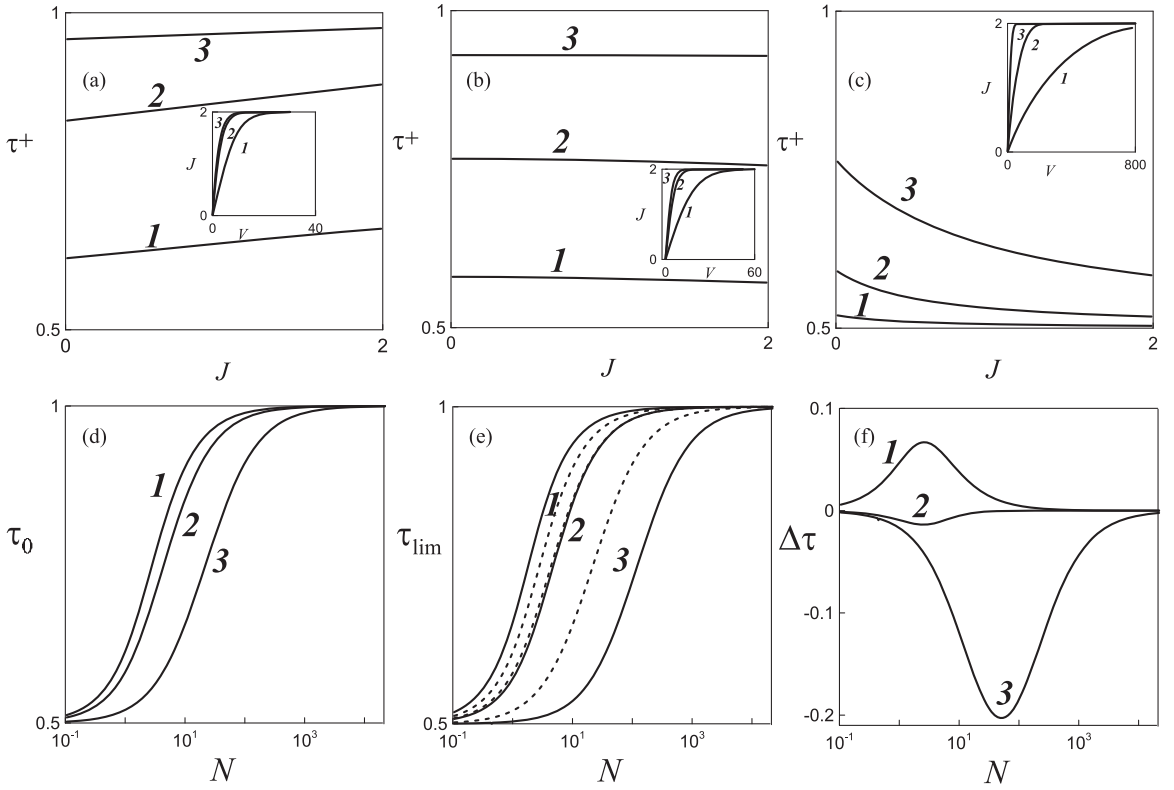

FIG. 2. Counterion transport number τ^+ versus salt flux J for varying enriched diffusion layer thickness L, (a) $L = 0.1$, (b) $L = 1$, and (c) $L = 10$; and membrane fixed charge density N, $N = 1$ (1), $N = 5$ (2), and $N = 25$ (3). Insets: voltage V versus J for the same values of L and N as in the main figure; (d) equilibrium counterion transport number τ_0 versus N for $L = 0.1$ (1), $L = 1$ (2), and $L = 10$ (3); (e) counterion transport number at the limiting current τ_{lim} (continuous line) and τ_0 (dashed line) versus N for $L = 0.1$ (1), $L = 1$ (2), and $L = 10$ (3); (f) $\Delta\tau = \tau_{\text{lim}} - \tau_0$ versus N for $L = 0.1$ (1), $L = 1$ (2), and $L = 10$ (3).

increase of the interface concentration at the enriched side of the membrane [dominating up to $N = O(L^2)$] is followed by a negative minimum of $\Delta\tau$ at $N \sim L^2$ and a subsequent growth of $\Delta\tau$ to zero in accordance with Eqs. (24) and (25).

III. HETEROGENEOUS CATION-EXCHANGE MEMBRANE

In this section we analyze the effect of CP on the counterionic transport number for a heterogeneous membrane in the three-layer setup of the previous section, as sketched in Fig. 4. The membrane is modeled as a periodic array of impermeable and ion-exchange parts. Mathematically, this yields the following formulation:

Diffusion layers (depleted layer $0 < x < 1$, $0 < y < 1$ and enriched layer $-L - 1 < x < 1$, $0 < y < 1$):

$$\nabla^2 c = 0, \quad \nabla(c\nabla\varphi) = 0. \tag{27}$$

Membrane ($-1 < x < 0$, $0.5 - h < y < 0.5 + h$):

$$\nabla(2\nabla c + N\nabla\varphi) = 0, \quad \nabla[(2c + N)\nabla\varphi] = 0. \tag{28}$$

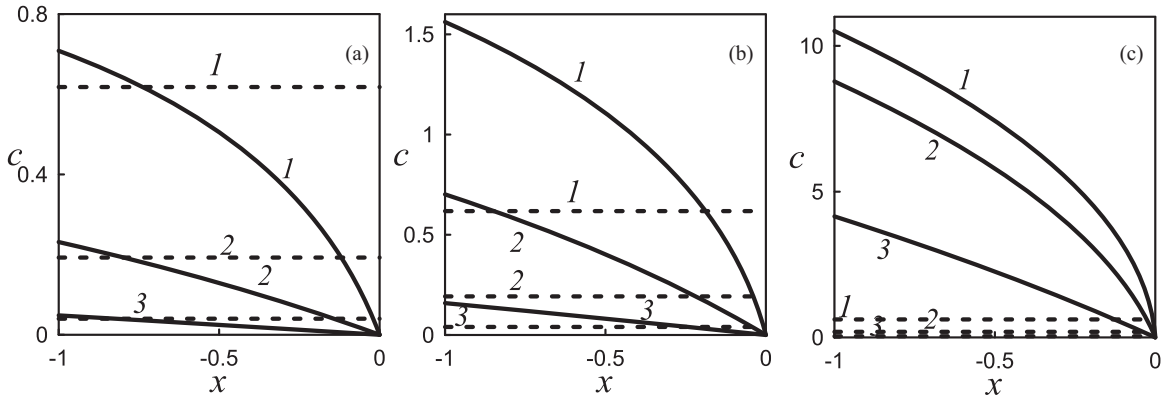

FIG. 3. Membrane coion concentration profiles for vanishing (dashed lines) and limiting (continuous lines) current: (a) $L = 0.1$, (b) $L = 1$, and (c) $L = 10$; and $N = 1$ (1), $N = 5$ (2), and $N = 25$ (3).

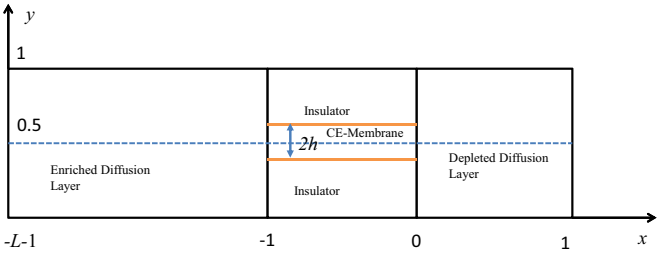

FIG. 4. (Color online) Sketch of three-layer setup for a heterogeneous cation-exchange membrane.

Continuity conditions at the membrane-solution interfaces ($x = -1,\ 0;\ 0.5 - h < y < 0.5 + h$):

$$\begin{aligned}(\ln c + \varphi)|_{x=-1-} &= (\ln[c+N] + \varphi)|_{x=-1+},\\ (\ln c - \varphi)|_{x=-1-} &= (\ln c - \varphi)|_{x=-1+};\end{aligned} \tag{29}$$

$$\begin{aligned}(\ln c + \varphi)|_{x=0+} &= (\ln[c+N] + \varphi)|_{x=0-},\\ (\ln c - \varphi)|_{x=0+} &= (\ln c - \varphi)|_{x=0-};\end{aligned} \tag{30}$$

$$\begin{aligned}(c_x + (c+N)\varphi_x)|_{x=-1-} &= (c_x + c\varphi_x)|_{x=-1+},\\ (c_x - c\varphi_x)|_{x=-1-} &= (c_x - c\varphi_x)|_{x=-1+};\end{aligned} \tag{31}$$

$$\begin{aligned}(c_x + (c+N)\varphi_x)|_{x=0+} &= (c_x + c\varphi_x)|_{x=0-},\\ (c_x - c\varphi_x|_{x=0+}) &= (c_x - c\varphi_x)|_{x=0-}.\end{aligned} \tag{32}$$

Vanishing fluxes at the symmetry lines and the impermeable part of the membrane:

$$\begin{aligned}&y = 0,1:\ c_y = \varphi_y = 0; \quad y = 0.5 \pm h,\\ &-1 < x < 0:\ c_y = \varphi_y = 0;\end{aligned} \tag{33}$$

$$x = -1,0, \quad y < 0.5 - h \quad \text{or} \quad y > 0.5 + h: c_x = \varphi_x = 0. \tag{34}$$

Outer edge conditions:

$$\begin{aligned}c(1,y) = c(-L-1,y) = 1;,\\ \varphi(1,y) = -V, \quad \varphi(-L-1,y) = 0.\end{aligned} \tag{35}$$

Of course the very same setup is suitable for modeling a micro- or nanochannel junction [26–28].

To allow for analytical treatment of the problem (27)–(35), let us neglect the transverse variation (y dependence) of the electric potential and ionic concentrations within the ion exchange channel, that is, let us assume

$$\begin{aligned}&-1 < x < 0, \quad 0.5 - h < y < 0.5 + h:\ c = c(x),\\ &\varphi = \varphi(x).\end{aligned} \tag{36}$$

Then, matching the ionic electrochemical potentials and ionic fluxes at the channel-solution interfaces $x = -1,0$ yields

$$\begin{aligned}x = -1-, 0+,\ 0.5 - h < y < 0.5 + h:\ c_x + c\varphi_x\\ = j^+ = \text{const},\ c_x - c\varphi_x = j^- = \text{const};\end{aligned} \tag{37}$$

$$\begin{aligned}&\ln c(-1-,0.5) + \varphi(-1-,0.5)\\ &\quad = \ln[c(-1+) + N] + \varphi(-1+),\end{aligned} \tag{38}$$

$$\ln c(0+,0.5) + \varphi(0+,0.5) = \ln[c(0-) + N] + \varphi(0-); \tag{39}$$

$$\ln c(-1-,0.5) - \varphi(-1-,0.5) = \ln c(-1+) + \varphi(-1+), \tag{40}$$

$$\ln c(0+,0.5) - \varphi(0+,0.5) = \ln c(0-) - \varphi(0-); \tag{41}$$

where $-j^+$ and $-j^-$ are the unknown cationic and anionic flux densities assumed constant across the interface.

Assumption (36) along with specifying the salt flux $-J = -(j^+ + j^-)$ result in splitting the problem (27)–(35) into the following three separate steps: (a) solving three decoupled problems for the ionic concentrations in the three separate regions corresponding to the diffusion layers and the membrane channel, (b) with the ionic concentration determined, computing the electric potential, and completing the solution through determining the dependence of the salt flux on the applied voltage.

(a) Computation of ionic concentrations.

Diffusion layers:

$$c = 1 + \frac{J}{4h} c_0(x,y). \tag{42}$$

Here, taking into account Eq. (37):

$$J = j^+ + j^- = 2\int_0^1 c_x dy, \tag{43}$$

whereas $c_0(x,y)$ is subject to determination from the solution of the following boundary-value problem:

$$\nabla^2 c_0 = 0, \quad -L-1 < x < -1 \quad \text{and} \quad 0 < x < 1, \quad 0 < y < 1; \tag{44}$$

$$c_0(1,y) = c_0(-L-1,y) = 0, \quad 0 < y < 1; \tag{45}$$

$$c_{0y}(x,0) = c_{0y}(x,1) = 0, \quad -L-1 < x < 1; \tag{46}$$

$$c_{0x}|_{x=-1,0} = 0, \quad 0 < y < 0.5 - h \quad \text{and} \quad 0.5 + h < y < 1; \tag{47}$$

$$c_{0x}|_{x=-1,0} = 1, \quad 0.5 - h < y < 0.5 + h. \tag{48}$$

The solution to this problem reads

$$c_0 = 2h(x-1) + \sum_{n=1}^{\infty} a_n \cos 2\pi n(y-0.5) \sinh 2\pi n(x-1), \quad 0 < x < 1; \tag{49}$$

$$c_0 = 2h(x+L+1) + \sum_{n=1}^{\infty} b_n \cos 2\pi n(y-0.5) \times \sinh 2\pi n(x+L+1), \quad -L-1 < x < -1; \tag{50}$$

where

$$a_n = \frac{\sin 2\pi nh}{(\pi n)^2 \cosh 2\pi n}; \quad b_n = \frac{\sin 2\pi nh}{(\pi n)^2 \cosh 2\pi nL}. \tag{51}$$

Membrane: Substituting condition (36) in Eqs. (28) yields

$$2c_x + \frac{NI}{2h(2c+N)} = \frac{J}{2h}, \quad -1 < x < 0, \tag{52}$$

where $-I$ is the total electric current,

$$I \stackrel{\text{def}}{=} 2\int_0^1 c\varphi_x|_{x=1} dx. \tag{53}$$

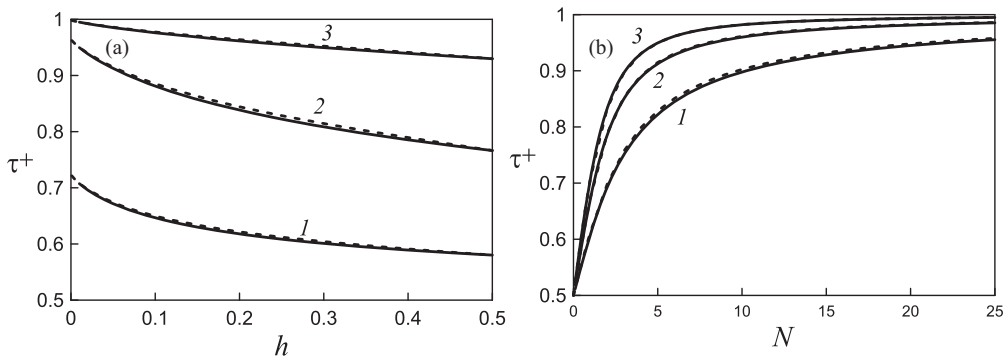

FIG. 5. (a) τ^+ versus channel width h for $N = 1$ (1), $N = 5$ (2), and $N = 25$ (3); and (b) τ^+ versus N for $h = 0.25$ (1), $h = 0.05$ (2), and $h = 0.01$ (3). τ^+ determined from the model (27)–(60) (continuous line) and τ^+ computed numerically in the full 2D model near equilibrium (dashed line).

Integrating Eq. (52) and applying boundary conditions (29) and (30) results in the following algebraic equation relating I to J:

$$\frac{J}{4h} = \left[c + \frac{NI}{2J}\ln\left(c + \frac{N}{2} - \frac{NI}{2J}\right)\right]\Bigg|_{-1+}^{0-}. \tag{54}$$

Here,

$$c|_{0-} = -\frac{N}{2} + \sqrt{\frac{N^2}{4} + \left[1 - \frac{J}{4h}\left(2h + \sum_1^\infty a_n \sinh 2\pi n\right)\right]^2}, \tag{55}$$

$$c|_{-1+} = -\frac{N}{2} + \sqrt{\frac{N^2}{4} + \left[1 + \frac{J}{4h}\left(2hL + \sum_1^\infty b_n \sinh 2\pi nL\right)\right]^2}. \tag{56}$$

(b) Computation of electric potential. Applying constancy of the flux densities at the channel-solution interface, $j^\pm$, defined by (37), we find

$$\begin{aligned} \varphi &= \frac{I}{J}\ln c, \quad 0 < x < 1; \\ \varphi &= \frac{I}{J}\ln c - V, \quad -L - 1 < x < -1. \end{aligned} \tag{57}$$

Assumption (36) reduces Eqs. (28) to their 1D version

$$2c_x + N\varphi_x = \frac{J}{2h}, \quad -1 < x < 0. \tag{58}$$

Integration of (58) along the permeable channel yields

$$N\varphi|_{-1+}^{0-} = A(J) \stackrel{\text{def}}{=} \frac{J}{2h} - 2c|_{-1+}^{0-}, \tag{59}$$

where $c|_{0-}$, $c|_{-1+}$ are specified by Eqs. (55) and (56).

Finally, making use of the boundary conditions (39) and (41), we find

$$V = \frac{A(J)}{N} + \ln\frac{c+N}{c}\Bigg|_{0-} - \ln\frac{c+N}{c}\Bigg|_{-1+} - \frac{I}{J}\ln\frac{4h - J\left(2h + \sum_1^\infty a_n \sinh 2\pi n\right)}{4hL + J\left(2h + \sum_1^\infty b_n \sinh 2\pi nL\right)}. \tag{60}$$

Numerical solution of the algebraic equations (54), with respect to I for a given J, yields the counterion transport number $\tau^+ = (J/I + 1)/2$. The calculation is completed by computing the voltage V for a given I through Eq. (60). The validity of this model is confirmed through comparing the transport number τ^+ determined from Eq. (54) with that computed numerically by solving the full problem (27–35) near equilibrium, $J \ll 1$, Fig. 5.

In Figs. 6(a)–6(c) we plot τ^+ versus J for varying N, L, and h. The limiting value $J^0 \leqslant 2$ of the salt flux corresponds to the vanishing of the solute concentration at the depleted interface at the channel axis $x = 0$, $y = 0.5$. The J^0 versus h dependence is plotted in Fig. 7(e). In columns (b) and (c) of Fig. 6, corresponding to symmetric diffusion layers (b) and a thick enriched diffusion layer (c) we observe the same general tendency: At equilibrium $J = 0$, τ^+ decreases upon the decrease of h, and from that value further decreases with increase of J.

The first effect is due to the increased control of the ionic fluxes by the membrane (mentioned in the previous section) upon decrease of the channel width. The smaller is the width of the channel the higher is the membrane resistance and, thus, the more it controls the overall permselectivity. Thus for a very narrow channel $h \ll 1$, according to Eq. (54) the counterion transport number in the heterogeneous three-layer setup approaches that of the membrane alone (dashed line in the first row in Fig. 6 corresponding to $h = 0.01$):

$$\tau^+ = \frac{1}{2}\left(1 + \frac{N}{\sqrt{N^2+4}}\right). \tag{61}$$

This value corresponds to the $L,l = 0$ limit in the expression

$$\tau^+ = \frac{1}{2}\left(1 + \frac{N}{\sqrt{N^2+4} + 2(L+l)}\right), \tag{62}$$

valid for a homogeneous setup. Here l is the dimensionless thickness of the depleted layer important in this context [for brevity, l is assumed unity elsewhere in this paper; for $l = 1$, Eq. (62) is identical with Eq. (24)].

The second effect, the decrease of permselectivity with development of CP for symmetric diffusion layers or a thick enriched diffusion layer is just an analog of the CP effect of the previous section (reproduced in row IV in Fig. 6 for

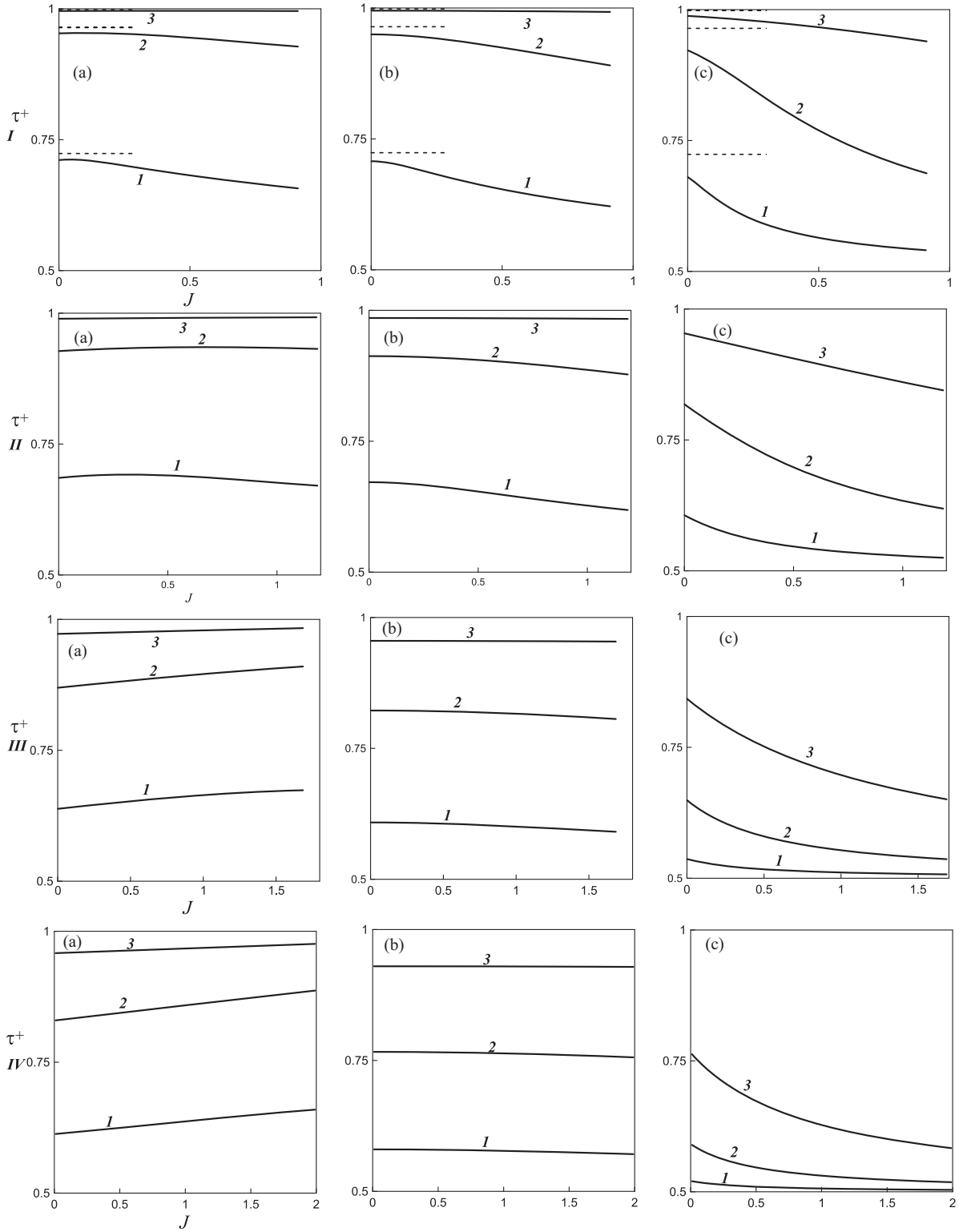

FIG. 6. τ^+ versus J for $h = 0.01$ (I), where dashed lines stand for the asymptotic value of τ^+ for $h \ll 1$, $h = 0.05$ (II), $h = 0.25$ (III), and homogeneous membrane $h = 0.5$ (IV); (a) $L = 0.1$, (b) $L = 1$, and (c) $L = 10$; $N = 1$ (1), $N = 5$ (2), and $N = 25$ (3).

comparison). While the first effect is the same also in column (a) in Fig. 6, corresponding to a thin enriched diffusion layer, the effect of CP is different and worthy of the following separate discussion.

In this column, upon increase of the channel width, we observe the reversal of the direction of variation of τ^+ with increase of J. This is due to flux focusing at the channel-solution interface which is the main qualitative footprint of heterogeneity in our system, illustrated in Fig. 7. In this figure we depict the interface salt concentration profiles $c(-1, y)$ and $c(0, y)$ for limiting salt flux J^0 (for a unit thickness of the depleted diffusion layer) solely dependent on the

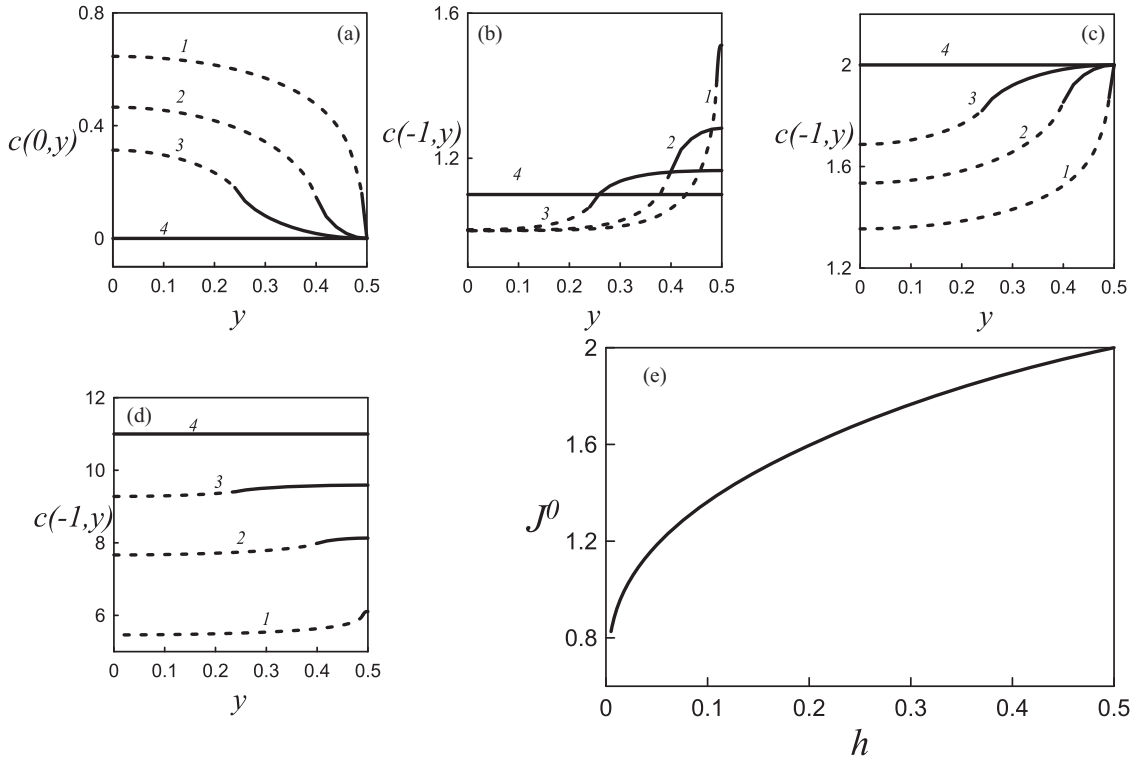

FIG. 7. Interface concentration profiles at the limiting current. (a) Depleted interface $x = 0+$; (b)–(d) enriched interface $x = -1-$ for (b) $L = 0.1$, (c) $L = 1$, and (d) $L = 10$. Continuous and dashed lines correspond to the interface concentration at the permselective and impermeable portions of the interface, respectively; (1) $h = 0.01$, (2) $h = 0.1$, (3) $h = 0.25$, and (4) $h = 0.5$. (e) Limiting salt flux J^0 versus h.

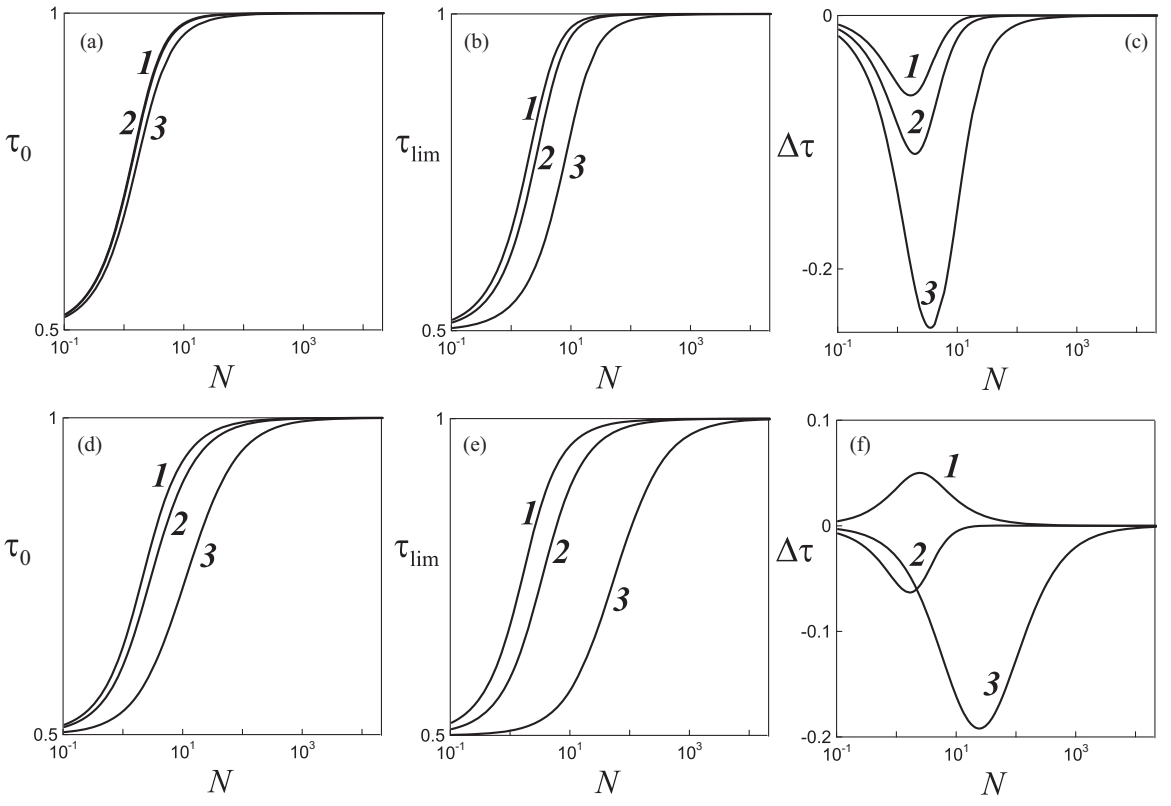

FIG. 8. τ_0 (a),(d) $\tau_{\rm lim}$ (b),(e), and $\Delta\tau$ (c),(f) versus N for $h = 0.01$ (a)–(c) and $h = 0.25$ (d)–(f). (1) $L = 0.1$, (2) $L = 1$, and (3) $L = 10$.

channel width h, Fig. 7(e), and varying channel width and thickness of the enriched diffusion layer. The essence of flux focusing is that the salt flux through the channel, J, is higher than its average over the entire membrane surface, $2hJ$. For a given channel width, the shorter is the respective diffusion layer, the more flux focusing affects the interface concentration.

Correspondingly, for a thin enriched diffusion layer, the drop in permselectivity due to increase of the interface concentration for maximal focusing at the minimal channel width (row I, Fig. 6) overtakes the opposite effect due to depletion, typical of a wide channel (nearly homogeneous membrane, row III, practically identical with row IV corresponding to a homogeneous membrane). The very same focusing effect also causes a steeper decrease of permselectivity in CP for a narrow channel than for a wide one in the symmetric case [column (b) in Fig. 6].

In Fig. 8 we summarize these findings through plotting the dependence of τ_0, $\tau_{\lim}$, and $\Delta\tau$ on N for varying h and L. For a wide channel [$h = 0.25$, Figs. 8(d)–8(f)] we observe the same general behavior as for a homogeneous membrane {compare with Figs. 2(d)–2(f)]. The only difference is the stronger depression of $\Delta\tau$ in the heterogeneous case, particularly pronounced in the symmetric case [compare plot (2) in Figs. 8(f) and 2(f)]. This is due to that fact that at the limiting current the depleted interface concentration at the channel axis is fixed at zero whereas the respective value at the enriched interface increases with the decrease of h, as illustrated in Figs. 7(a)–7(c). For a narrow channel [$h = 0.01$, Fig. 8(c)] this effect is particularly strong, yielding a reversal of the $\Delta\tau$ dependence on N for a thin enriched diffusion layer [compare plot 1 in Fig. 8(c) to the same plots in Figs. 8(f) and 2(f)].

IV. CONCLUSIONS

In the three-layer setups analyzed, the counterionic transport number strongly depends on the electric current due to the interface concentration variation in the course of CP. For a homogeneous membrane, the main observations may be summarized as follows:

Highly permselective membrane. With the depleted layer thicker than the enriched one, the decrease of permselectivity with concentration polarization is insignificant due to the fact that at the depleted interface the permselectivity does not increase because it is high to begin with, whereas at the enriched interface the concentration variation is small. On the other hand, with the enriched diffusion layer thicker than the depleted one, a considerable loss of overall permselectivity may occur, the bigger the larger is the ratio of the diffusion layer thicknesses. Thus, for a thick enriched diffusion layer the main mechanism of counterion transport number reduction with concentration polarization is the increasing asymmetry between the minor gain of permselectivity at the depleted interface and its major loss at the enriched one.

Poorly permselective membrane. Variation of salt concentration across the membrane and its related variation of conductivity result in the nonconstancy of the electric field. This, in turn, results in increased convexity of the salt concentration profile in the membrane and a related drop of permselectivity.

For a heterogeneous membrane, the aforementioned effects interact, with the effect of flux focusing at the entrance to and the exit from the channel. The thinner is the corresponding diffusion layer, the stronger is the latter effect, amounting to the increase of the effective flux through the channel compared to the nominal average flux through the overall membrane surface.

The purely electrostatic model analyzed in this paper constitutes a "kinematic" step towards comprehensive understanding of the effects of CP on permselectivity. Numerous effects inherent in CP, such as water splitting and possible variations of the membrane charge [10,14], left beyond the scope of our analysis, should be addressed in future studies.

ACKNOWLEDGMENT

The work was supported by the USA-Israel Binational Science Foundation (Grant No. 2010199).

[1] V. G. Levich, *Physicochemical Hydrodynamics* (Prentice-Hall, Englewood Cliffs, NJ, 1962).
[2] K. S. Spiegler, Desalination **9**, 367 (1971).
[3] H. Strathmann, *Ion-Exchange Membrane Separation Processes* (Elsevier, Amsterdam, 2004).
[4] V. J. Frillete, J. Phys. Chem. **61**, 168 (1957).
[5] M. Block and J. A. Kitchener, J. Electrochem. Soc. **113**, 947 (1966).
[6] R. Simons, Desalination **29**, 41 (1979).
[7] R. Simons, Nature (London) **280**, 824 (1979).
[8] I. Rubinstein and B. Zaltzman, Phys. Rev. E **62**, 2238 (2000).
[9] E. V. Dydek, B. Zaltzman, I. Rubinstein, D. S. Deng, A. Mani, and M. Z. Bazant, Phys. Rev. Lett. **107**, 118301 (2011).
[10] E. V. Dydek and M. Z. Bazant, AIChE J. **59**, 3539 (2013)..
[11] D. S. Deng, E. V. Dydek, J.-H. Han, S. Schlumpberger, A. Mani, B. Zaltzman, and M. Z. Bazant, Langmuir **29**, 16167 (2013).
[12] A. Yaroshchuk, E. Zholkovskiy, S. Pogodin, and V. Baulin, Langmuir **27**, 11710 (2011).
[13] A. E. Yaroshchuk, Adv. Colloid Interface Sci. **168**, 278 (2011).
[14] M. B. Andersen, M. van Soestbergen, A. Mani, H. Bruus, P. M. Biesheuvel, and M. Z. Bazant, Phys. Rev. Lett. **109**, 108301 (2012).
[15] N. Lakshminarayanaiah, *Transport Phenomena in Memebranes* (Academic Press, New York, 1969).
[16] M. Taky, G. Pourcelly, F. Lebon, and C. Gavach, J. Electroanal. Chem. **336**, 171 (1992).
[17] J. J. Krol, M. Wessling, and H. Strathmann, J. Membr. Sci. **162**, 145 (1999).
[18] X. T. Le, J. Membr. Sci. **397**, 66 (2012).
[19] J. Schiffbauer and G. Yossifon, Phys. Rev. E **86**, 056309 (2012).
[20] I. Rubinstein, Phys. Fluids **3**, 2301 (1991).
[21] I. Rubinstein, B. Zaltzman, and T. Pundik, Phys. Rev. E **65**, 041507 (2002).

[22] A. S. Khair, Phys. Fluids **23**, 072003 (2011).
[23] T. Teorell, Proc. Soc. Exp. Biol. Med. **33**, 282 (1935).
[24] K. H. Meyer and J. F. Sievers, Helv. Chem. Acta **19**, 649 (1936).
[25] R. Roy and F. W. J. Olver, in *NIST Handbook of Mathematical Functions*, edited by F. W. J. Olver, D. M. Lozier, R. F. Boisvert, *et al*. (Cambridge University Press, New York, 2010).
[26] S. J. Kim, Y. C. Wang, J. H. Lee, H. Jang, and J. Han, Phys. Rev. Lett. **99**, 044501 (2007).
[27] T. A. Zangle, A. Mani, and J. G. Santiago, Chem. Soc. Rev. **39**, 1014 (2010).
[28] G. Yossifon and H.-C. Chang, Phys. Rev. Lett. **101**, 254501 (2008).